

## References and Notes

1. M. Elliot *et al.*, *Paleoceanography* **13**, 433 (1998).
2. R. F. Scott, *Geogr. J.* **25**, 353 (1905).
3. J. T. Hollin, *J. Glaciol.* **32**, 173 (1962).
4. A. Penck, *Sitzungsber. Preuss. Akad. Wiss. Berlin Phys.-Math. Kl.* **6**, 76 (1928).
5. J. B. Anderson, S. S. Shipp, A. L. Lowe, J. S. Wellner, A. B. Mosola, *Quat. Sci. Rev.* **21**, 49 (2002).
6. H. Conway, B. L. Hall, G. H. Denton, A. M. Gades, E. D. Waddington, *Science* **286**, 280 (1999).
7. S. Anandakrishnan, D. E. Voigt, R. B. Alley, M. A. King, *Geophys. Res. Lett.* **30**, 1361 (2003).
8. The increase in pressure opposing ice flow from the rising tide is more important than the decrease in basal friction as the rising tide floats ice off of its bed, contrary to the expectation of the simplest model, in which the spreading tendency of grounded (nonfloating) ice is restrained by basal friction. If the forcing and the resulting slowdown were sustained, thickening and grounding-line advance would result from the sea-level rise.
9. M. Meier, A. Post, *J. Geophys. Res.* **92**, 9051 (1987).
10. S. Anandakrishnan, G. A. Catania, R. B. Alley, H. J. Horgan, *Science* **315**, 1835 (2007); published online 1 March 2007 (10.1126/science.1138393).
11. T. K. Dupont, R. B. Alley, *Geophys. Res. Lett.* **32**, L04503 (2005).
12. H. J. Horgan, S. Anandakrishnan, *Geophys. Res. Lett.* **33**, L18502 (2006).
13. A. B. Mosola, J. B. Anderson, *Quat. Sci. Rev.* **25**, 2177 (2006).
14. B. Kamb, in *The West Antarctic Ice Sheet: Behavior and Environment*, R. B. Alley, R. A. Bindshadler, Eds. (American Geophysical Union, Washington, DC, 2001), pp. 157–199.
15. S. T. Rooney, D. D. Blankenship, R. B. Alley, C. R. Bentley, in *Geological Evolution of Antarctica*, M. R. A. Thomson, J. A. Crame, J. W. Thompson, Eds. (Cambridge Univ. Press, Cambridge, 1991), pp. 261–265.
16. B. R. Parizek, R. B. Alley, *Global Planet. Change* **42**, 265 (2004).
17. Materials and methods are available as supporting material on Science Online.
18. A sediment wedge with a rise of 31 m over 8 km and then a fall of 31 m over 3.2 km is typical of the reference experiment; however, because the sediment was added beneath an equilibrated ice shelf and the different models give slightly different equilibrium shelves, the sediment wedges differ somewhat between the models.
19. To good approximation, for a sediment deposit of maximum height  $h$  filling a sub-ice-shelf cavity of constant angle  $\theta$ , relative to the horizontal bed, and with constant angle  $\phi$ , the sediment volume per unit of width is  $V = (\cot \theta + \cot \phi)h^2/2$ , and the volume increment  $dV$  to thicken by  $dh$  increases linearly with the wedge thickness as  $dV = (\cot \theta + \cot \phi)hdh$ .
20. G. K. C. Clarke, *Annu. Rev. Earth Planet. Sci.* **33**, 247 (2005).
21. J. Weertman, *J. Glaciol.* **13**, 3 (1974).
22. Bedrock bumps have the same effect as soft-sediment wedges and are much more likely to be encountered by a retreating grounding line than are sediment wedges. As shown in (12), soft-sediment wedges are formed at the grounding line during retreat and may be encountered on readvance, but they are unlikely to survive being overrun by advancing ice, so as to exist beneath grounded ice to influence grounding-line retreat.
23. R. B. Alley *et al.*, *Geomorphology* **75**, 76 (2006).
24. T. K. Dupont, R. B. Alley, *Geophys. Res. Lett.* **33**, L09503 (2006).
25. For sufficiently extensive ice shelves, a 5% decrease in buttressing will require a >5% decrease in the side-drag area.
26. E. Rignot, S. S. Jacobs, *Science* **296**, 2020 (2002).
27. T. A. Scambos, J. A. Bohlander, C. A. Shuman, P. Skvarca, *Geophys. Res. Lett.* **31**, L18402 (2004).
28. J. A. Dowdeswell, A. Elverhoi, *Mar. Geol.* **188**, 3 (2002).
29. J. S. Wellner, D. C. Heroy, J. B. Anderson, *Geomorphology* **75**, 157 (2006).
30. P. Huybrechts, *Quat. Sci. Rev.* **21**, 203 (2002).
31. J. F. Adkins, K. McIntyre, D. R. Schrag, *Science* **298**, 1769 (2002).
32. We thank J. Anderson, H. Horgan, S. Jacobs, D. Voigt, P. Burkett, and other colleagues. Partial funding was provided by NSF through grants (including 0424589, 0440447, 0440899, 0531211, 0447235, and 0539578) and by the Gary Comer Science and Education Foundation

## Supporting Online Material

www.sciencemag.org/cgi/content/full/1138396/DC1

Materials and Methods

References and Notes

4 December 2006; accepted 21 February 2007

Published online 1 March 2007;

10.1126/science.1138396

Include this information when citing this paper.

# Permissive and Instructive Anterior Patterning Rely on mRNA Localization in the Wasp Embryo

Ava E. Brent, Gozde Yucel, Stephen Small, Claude Desplan\*

The long-germ mode of embryogenesis, in which segments arise simultaneously along the anterior-posterior axis, has evolved several times in different lineages of the holometabolous, or fully metamorphosing, insects. *Drosophila*'s long-germ fate map is established largely by the activity of the dipteran-specific Bicoid (Bcd) morphogen gradient, which operates both instructively and permissively to accomplish anterior patterning. By contrast, all nondipteran long-germ insects must achieve anterior patterning independently of *bcd*. We show that *bcd*'s permissive function is mimicked in the wasp by a maternal repression system in which anterior localization of the wasp ortholog of *giant* represses anterior expression of the trunk gap genes so that head and thorax can properly form.

The highly conserved segmented insect body plan is achieved by great flexibility in developmental mechanisms. In the ancestral short-germ mode of embryogenesis, head and thorax arise from the egg's posterior, and abdominal segments emerge progressively from a posterior growth zone. By contrast, in the more derived long-germ mode, all segments form simultaneously in a syncytial environment, with head and thorax at the egg's anterior. Long-germ development has evolved several times in different holometabolous insect lineages (1), includ-

ing the Diptera, of which the most extensively studied member is *Drosophila melanogaster* (*Dm*). A morphogen gradient of Bicoid (Bcd) protein, formed by translation from a maternal, anteriorly localized mRNA source, establishes the *Drosophila* body plan. Embryos derived from *bcd* mutant mothers lack head, thorax, and some abdominal segments (2, 3).

Despite its critical role in patterning the *Drosophila* long-germ embryo, *bcd* is distinctive to the higher Diptera (4). Thus, all other insects, including long-germ nondipterans, must employ a *bcd*-independent mechanism to accomplish segmentation. To identify such a mechanism, we investigated anterior patterning in the hymenopteran parasitoid wasp, *Nasonia vitripennis* (*Nv*) (5). The embryonic fate map of this independently evolved (6) long-germ insect is essentially identical to that

of *Drosophila*, except that it is formed in the absence of *bcd*. We previously showed that in the early *Nasonia* embryo, *bcd*'s morphogenetic activity is performed by *orthodenticle1* (*Nv-otd1*), the ortholog of the *Drosophila bcd* target gene, *Dm-otd* (5). Although strictly zygotic in *Drosophila*, *Nv-otd1* mRNA is maternally provided and localized to both oocyte poles, resulting in bipolar protein gradients. The anterior *Nv-otd1* gradient regulates expression of zygotic head and thoracic gap genes, including the *Nasonia* orthologs of the *bcd* targets, *giant* (*gt*), and *hunchback* (*hb*) (5).

In addition to instructively activating the genes that pattern the head and thorax, *bcd* also functions permissively in *Drosophila* to indirectly repress posteriorly acting genes, such as the trunk gap genes, that would otherwise inhibit anterior development (7). We show here that *Nasonia* accomplishes this task by further employing maternal mRNA localization to position a repressor of trunk development at the anterior, thereby allowing formation of the head and thorax.

In the *Drosophila* embryo, the gap gene *Krüppel* (*Dm-Kr*) is expressed in a broad central stripe (Fig. 1A) and is required for formation of thoracic segment 1 (T1) through abdominal segment 5 (A5) (8). The positioning of *Kr* and, hence, of the trunk, is established by *bcd* and the terminal system; in embryos derived from *bcd* mutant mothers, the *Dm-Kr* domain broadens and shifts anteriorly (Fig. 1B) (7, 9). *bcd*'s zygotic targets, *Dm-hb* and *Dm-gt*, mediate this regulation; in single *Dm-hb* (7, 9) or *Dm-gt* mutant embryos (Fig. 1C), *Dm-Kr* shows slight anterior expansion (10), and in embryos mutant for both, *Dm-Kr*'s anterior shift is comparable to that seen from loss of *bcd* alone (11). However,

New York University, Department of Biology, Center for Developmental Genetics, 100 Washington Square East, New York, NY 10003, USA.

\*To whom correspondence should be addressed. E-mail: cd38@nyu.edu

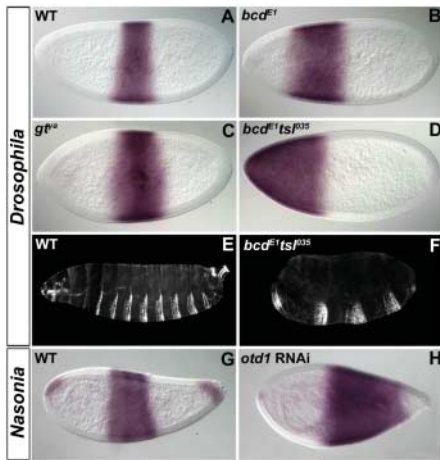


**Fig. 1.** Regulation of *Kr* in *Drosophila* and *Nasonia*. *Dm-Kr* expression in embryos that are wild-type (A), lacking *Dm-bcd* (B), mutant for *Dm-gt* (C), or lacking *Dm-bcd* and *Dm-tsl* (D). (E) Wild-type or (F) *Dm-bcd;tsl* cuticle. Cellular blastoderm expression of *Nv-Kr* in wild-type embryos (G) or after *Nv-otd1* RNAi (H).

*Dm-Kr* does not reach the anterior tip of the embryo because of additional repression by the terminal system; in embryos lacking *bcd* and *torsolike* (*Dm-tsl*), *Dm-Kr* expands throughout the anterior (Fig. 1D), resulting in embryos with as few as four abdominal segments (Fig. 1, E and F) (7).

To determine how the *Nasonia* embryo's trunk is positioned, we isolated the *Nasonia* ortholog of *Kr* and found that it was expressed in a central gap-like domain (Fig. 1G). To confirm that *Nv-Kr* was acting as a gap gene, we knocked down *Nv-Kr* using parental RNA interference (RNAi) (5, 12) and observed a gap phenotype: loss of T3 and A1 to A4. We hypothesized that because *Nv-otd1* performs other *bcd* functions, the *otd1* anterior morphogenetic gradient might be functioning to position *Nv-Kr*. However, after *Nv-otd1* RNAi, we found that although *Nv-Kr* expanded posteriorly, the anterior boundary was unaffected (Fig. 1H).

We next asked whether one of *bcd*'s zygotic gap gene targets could be implicated in *Nv-Kr* anterior boundary formation. Our analysis of *Nv-gt* revealed an essential role in repressing *Nv-Kr*. In *Drosophila*, *Dm-gt* is expressed in two regions, a posterior stripe and a *bcd*-activated anterior domain (13). *Nv-gt* expression in cellularized embryos was similar (Fig. 2E); however, we found *Nv-gt* expressed maternally at earlier stages. In freshly laid embryos, *Nv-gt* mRNA occupied a broad anterior gradient, with highest levels at the anterior pole (Fig. 2A). This domain persisted through pole cell formation (Fig. 2B) and syncytial blastoderm stages (Fig. 2C), intensifying at the onset of cellularization simultaneously with the appearance of a posterior cap, marking commencement of zygotic expression (Fig. 2D). During cellularization, *Nv-gt* expression resolved into zygotic anterior and posterior gap domains (Fig. 2E), which are regulated by *Nv-otd1* (5). To confirm that the early *Nv-gt* expression we had ob-

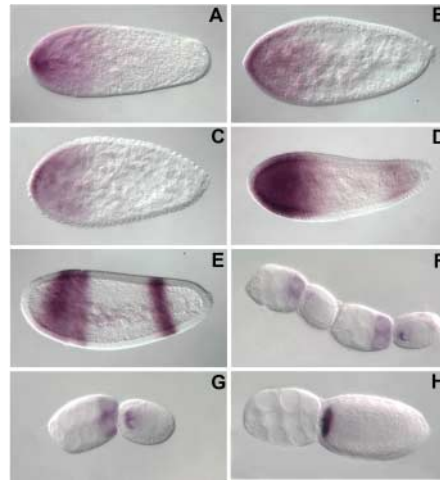


**Fig. 2.** Expression of maternal and zygotic *Nv-gt* during *Nasonia* oogenesis and embryogenesis. Maternal *Nv-gt* mRNA in freshly laid embryos (A), during pole cell formation (B), and in the syncytial blastoderm (C). Zygotic *Nv-gt* expression at onset of cellularization (D) and in the cellular blastoderm (E). Maternal anterior localization during oocyte development (F to H).

served was maternal, we examined egg chambers and detected *Nv-gt* in the nurse cells and in the oocyte, where it accumulated around the nucleus (Fig. 2F). In mature oocytes, *Nv-gt* was localized to the anterior pole (Fig. 2G), ultimately assuming a tight anterior localization pattern (Fig. 2H).

Having established that *Nv-gt* is maternally provided and anteriorly localized, we used RNAi to determine its role during segmentation. Knockdown of *Nv-gt* resulted in unhatched larvae, all arrested with the same phenotype: complete loss of head and thoracic (T1-T3) segments (Fig. 3, A and B). In addition, A6 and A7 showed fusions and deletions due to loss of posterior zygotic *Nv-gt* (Fig. 3B). Anterior defects were also visible at earlier stages in knockdown embryos; analysis of *engrailed* (*Nv-en*) revealed anterior truncations (Fig. 3, C and D), whereas Ultrabithorax/AbdominalA (*Ubx/AbdA*) expression showed that all remaining tissue was abdominal (Fig. 3, E and F). The *Nv-gt* RNAi anterior phenotype was more severe than that of *Dm-gt* null mutations, in which anterior defects are limited to loss of labial and labral structures (13). By contrast, knockdown of *Nv-gt* resembled the all-abdominal phenotype observed in *Drosophila* embryos lacking both *bcd* and *Dm-tsl* (Fig. 1F).

In *Drosophila*, it has been shown that *Dm-gt* and *Dm-Kr* mutually repress each other, a relationship that defines the embryo's center (10, 11). To determine whether *Nv-gt* also regulates *Nv-Kr*, we examined *Nv-Kr* expression in *Nv-gt* RNAi embryos and found dramatic expansion of *Nv-Kr* to the anterior pole (Fig. 3, G and H), indicating a major role for *Nv-gt* in setting the *Nv-Kr* anterior boundary. Moreover, loss of zygotic *Nv-gt* alone did not result in anterior *Nv-Kr* expansion. As noted earlier, the anterior *Nv-Kr* border was unaffected by

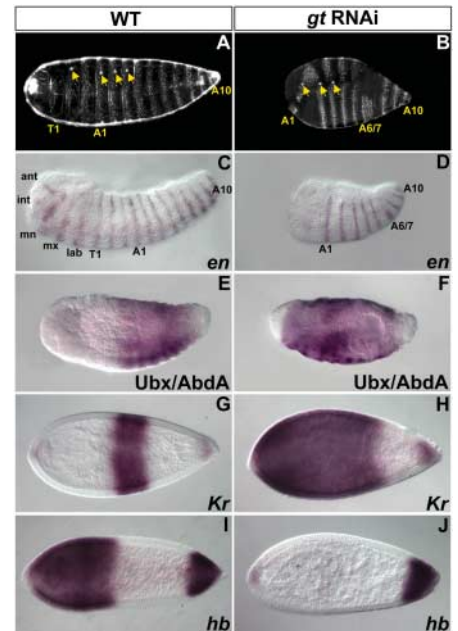


**Fig. 3.** Knockdown of *Nv-gt* in *Nasonia* results in anterior deletions. Wild-type (A) and *Nv-gt* RNAi (B) cuticles. Yellow arrows indicate spiracles on T2, A1 to A3. Expression of *Nv-en* (C and D), *Nv-Kr* (G and H), and *Nv-hb<sub>zyg</sub>* (I and J) in wild-type [(C), (G), and (I)] and *Nv-gt* RNAi [(D), (H), and (J)] embryos. *Ubx/AbdA* protein expression in wild-type (E) and *Nv-gt* RNAi (F) embryos.

*Nv-otd1* RNAi (Fig. 1H), whereas zygotic *Nv-gt* was eliminated (5). Thus, maternal *Nv-gt* appears to be the main repressor of *Nv-Kr*, mimicking both *bcd* and the terminal system in *Drosophila*.

The absence of head and thorax after *Nv-gt* RNAi was also similar to the phenotype of the *Nasonia* zygotic *hb* mutant *headless* (14). To investigate this correlation, we examined zygotic *Nv-hb* expression after *Nv-gt* RNAi and observed loss of the anterior *Nv-hb* domain (Fig. 3, I and J), suggesting that the anterior deletions seen in *Nv-gt* RNAi embryos were caused by loss of zygotic *Nv-hb*. Our observations generated two models for *Nv-gt* function: Either maternally localized *Nv-gt* activates expression of anterior zygotic *Nv-hb* (Fig. 4A), or *Nv-gt* negatively regulates a *hb*-repressor (Fig. 4A). Because *Dm-Gt* principally acts as a repressor (15), we favored the second model, hypothesizing that *Nv-Kr* might be the *hb*-repressor (Fig. 4A). In support of this model, we observed that the anterior and posterior zygotic *Nv-hb* domains expanded toward the center in *Nv-Kr* RNAi embryos (Figs. 3I and 4C). This double-repressor model for head and thorax patterning circumscribes maternally localized *Nv-gt* function solely to the repression of *Nv-Kr*.

To test this model, we asked whether expansion of *Nv-Kr* into the developing head and thoracic region causes deletion of those segments. If so, we would expect to see anterior patterning restored in embryos lacking *Nv-gt* and *Nv-Kr*. As a control for double RNAi, we examined embryos from females knocked down for

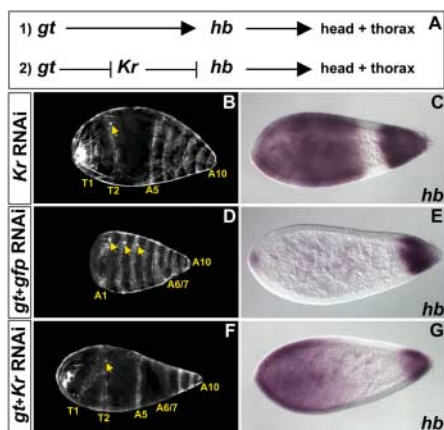


**Fig. 4.** Repression of *Nv-Kr* by maternal *Nv-gt* is required for head and thorax formation in *Nasonia*. (A) Two models for maternal *Nv-gt* function. Cuticular analysis (B, D, and F) and *Nv-hb<sub>zyg</sub>* expression (C, E, and G) after knockdown for *Nv-Kr* [(B) and (C)], *Nv-gt+gfp* [(D) and (E)], and *Nv-gt+Kr* [(F) and (G)].

*Nv-gt* and green fluorescent protein (*gfp*) and observed the expected *Nv-gt* phenotype: deletion of head and thorax, as well as loss of anterior *Nv-hb* expression (Fig. 4, D and E). Knockdown of *Nv-gt* and *Nv-Kr* yielded striking results. In 92% of examined embryos, the head and thorax (T1/T2) were restored (Fig. 4F), and the resulting cuticular phenotypes were essentially identical to those after *Nv-Kr* RNAi alone (Fig. 4B). Consistent with rescued head and thorax development, anterior zygotic *Nv-hb* was also restored, although not to wild-type levels (Fig. 4G). Nonetheless, the amount of *Nv-hb* present in *Nv-gt+Kr* RNAi embryos was sufficient to direct head and thorax development, demonstrating that *Nv-Kr* expansion impedes anterior patterning and that maternally localized *Nv-gt* confines *Nv-Kr* to the embryo's center. Thus, whereas in *Drosophila*, *bcd*-activated *Dm-gt* plays only a moderate role in positioning *Nv-Kr* (Fig. 1C), in *Nasonia*, maternal *Nv-gt* is sufficient to perform this function. This distinction led us to consider whether *Dm-gt*'s role in *Drosophila* would be enhanced if the *Drosophila* embryo were reengineered to develop like *Nasonia*—with *Dm-gt* maternally provided and anteriorly localized. We found that, whereas *Dm-gt* was sufficient to repress *Dm-Kr* anteriorly in the absence of *bcd* (fig. S1B), head and thoracic structures were not rescued (fig. S1C)—an unsurprising result given that, in addition to permitting anterior development by regulating *Kr*-repressing gap genes, *bcd* also functions instructively to activate genes required for head and thorax formation. In *Nasonia*, by contrast, the instructive and permissive anterior patterning functions are discrete. Head- and thorax-specific genes are triggered by an instructive anterior determinant, maternal *Nv-otd1*, which is localized independently of the permissively acting maternal repression system, *Nv-gt*.

A comparison of the molecular mechanisms employed by two independently evolved (6) long-

germ insects not only uncovers those features essential to this developmental mode but also sheds light on how the *bcd*-dependent anterior patterning program might have evolved. Through analysis of the regulation of the trunk gap gene *Kr* in *Drosophila* and *Nasonia*, we have been able to demonstrate that anterior repression of *Kr* is essential for head and thorax formation and is a common feature of long-germ patterning. Both insects accomplish this task through maternal, anteriorly localized factors that either indirectly (*Drosophila*) or directly (*Nasonia*) repress *Kr* and, hence, trunk fates. In *Drosophila*, the terminal system and *bcd* regulate expression of gap genes, including *Dm-gt*, that repress *Dm-Kr*. *Nasonia*'s *bcd*-independent long-germ embryos must solve the same problem, but they employ a maternally localized repression system in which maternal *Nv-gt* is localized to the oocyte's anterior, where it represses *Nv-Kr*. In the dipteran lineage, whereas *gt* retained the ability to repress *Kr*, maternal regulation of *Kr*'s position was taken over by two novel features—*bcd*, a specific dipteran innovation, and the terminal pathway, which, although present ancestrally, appears to function less extensively in the anterior of non-dipteran insects (16, 17). In addition to activating anterior patterning genes such as *otd* and *hb*, *bcd* also acquired regulation of *gt*, which became a strictly zygotic gene with a reduced role in repressing *Kr*. Our findings thus identify two independent mechanisms for long-germ anterior patterning—one using two maternally localized genes, *otd1* and *gt*, that respectively activate anterior zygotic patterning genes and repress trunk fates, and a second using *bcd* for these same functions, thereby demoting *otd* and *gt* to zygotic gap genes. Interestingly, it appears that long-germ embryos use RNA localization for a number of different developmental processes (5, 18, 19). By contrast, in short-germ insects, although some localized RNAs have been identified, there is as yet no evidence of their contribution to anterior-posterior patterning (20).

mRNA localization indeed appears to be an important component of long-germ embryogenesis, perhaps even playing a role in the transition from the ancestral short-germ to the derived long-germ fate.

#### References and Notes

- G. K. Davis, N. H. Patel, *Annu. Rev. Entomol.* **47**, 669 (2002).
- T. Berleth *et al.*, *EMBO J.* **7**, 1749 (1988).
- W. Driever, C. Nusslein-Volhard, *Cell* **54**, 83 (1988).
- J. Lynch, C. Desplan, *Curr. Biol.* **13**, R557 (2003).
- J. A. Lynch, A. E. Brent, D. S. Leaf, M. A. Pultz, C. Desplan, *Nature* **439**, 728 (2006).
- J. Savard *et al.*, *Genome Res.* **16**, 1334 (2006).
- G. Struhl, P. Johnston, P. A. Lawrence, *Cell* **69**, 237 (1992).
- A. Preiss, U. B. Rosenberg, A. Kienlin, E. Seifert, H. Jackle, *Nature* **313**, 27 (1985).
- M. Hulskamp, C. Pfeifle, D. Tautz, *Nature* **346**, 577 (1990).
- X. Wu, R. Vakani, S. Small, *Development* **125**, 3765 (1998).
- R. Kraut, M. Levine, *Development* **111**, 611 (1991).
- J. A. Lynch, C. Desplan, *Nat. Protocols* **1**, 486 (2006).
- R. Kraut, M. Levine, *Development* **111**, 601 (1991).
- M. A. Pultz *et al.*, *Development* **132**, 3705 (2005).
- G. F. Hewitt *et al.*, *Development* **126**, 1201 (1999).
- J. A. Lynch, E. C. Olesnick, C. Desplan, *Dev. Genes Evol.* **216**, 493 (2006).
- R. Schroder, C. Eckert, C. Wolff, D. Tautz, *Proc. Natl. Acad. Sci. U.S.A.* **97**, 6591 (2000).
- E. C. Olesnick *et al.*, *Development* **133**, 3973 (2006).
- A. Bashirullah, R. L. Cooperstock, H. D. Lipshitz, *Annu. Rev. Biochem.* **67**, 335 (1998).
- G. Bucher, L. Farzana, S. J. Brown, M. Klingler, *Evol. Dev.* **7**, 142 (2005).
- The authors wish to thank members of the Desplan and Small laboratories for support and advice. This project was supported by NIH grants GM64864, awarded to C.D., and GM51946, awarded to S.S. A.E.B. is a Damon Runyon Fellow, supported by the Damon Runyon Cancer Research Foundation (DRG-1870-05).

#### Supporting Online Material

www.sciencemag.org/cgi/content/full/315/5820/1841/DC1  
Materials and Methods

SOM Text

Fig. S1

References

13 November 2006; accepted 7 March 2007

10.1126/science.1137528

## Emergent Biogeography of Microbial Communities in a Model Ocean

Michael J. Follows,<sup>1\*</sup> Stephanie Dutkiewicz,<sup>1</sup> Scott Grant,<sup>1,2</sup> Sallie W. Chisholm<sup>3</sup>

A marine ecosystem model seeded with many phytoplankton types, whose physiological traits were randomly assigned from ranges defined by field and laboratory data, generated an emergent community structure and biogeography consistent with observed global phytoplankton distributions. The modeled organisms included types analogous to the marine cyanobacterium *Prochlorococcus*. Their emergent global distributions and physiological properties simultaneously correspond to observations. This flexible representation of community structure can be used to explore relations between ecosystems, biogeochemical cycles, and climate change.

A significant challenge in understanding the changing earth system is to quantify and model the role of ocean ecosystems in the global carbon cycle. The structure of microbial communities in the surface ocean is

known to regulate important biogeochemical pathways, including the efficiency of export of organic carbon to the deep ocean. Although there is extraordinary diversity in the oceans, the biomass of local microbial communities at